MINERALOGIA POLONICA
Vol. 17, No 1—1986

Marek MUSZYŃSKI, Piotr WYSZOMIRSKI**

ADULARIA FROM THE BASEMENT OF THE CRACOW--SILESIAN MONOCLINE NEAR ZAWIERCIE

Abstract. Macro- and microscopic studies, as well as X-ray, IR spectroscopic and electron microprobe investigations were carried out on adularias from veinlets crosscutting the altered sedimentary rocks of the basement of the Cracow-Silesian monocline near Zawiercie. It was found that they are minerals varying in the degree of order — from low to intermediate. The content of the Ab component ranges from 1.5 to 2.5% (occasionally up to 4%), while that of the An component is generally less than 1%. A characteristic feature of the adularia crystals studied is the presence of diadochic admixtures of barium, averaging 0.1—0.3 wt.% BaO, but sporadically running up to 1 wt.% BaO. The adularia studied is another, after baryte, mineral from the basement of the Cracow--Silesian monocline that shows a concentration of barium.

INTRODUCTION

The rocks of the sub-Devonian basement of the Cracow-Silesian monocline are crosscut by a complex network of veinlets of different age and varying mineralogical composition. About 100 minerals have been identified in them so far, over 75% in this number being ore minerals of Fe, Cu, Mo, Zn, Pb, Bi, W, Ag, Au, Co, Ni and As.

Adularia is a common component of fissure veinlets and rocks subject to potassium metasomatism. It was found in 11 out of 23 boreholes studied. Adularia was reported by many investigators, mainly from altered sedimentary rocks older than the Devonian (Łydka 1971, 1973; Ciemniewska 1978; Harańczyk 1978; Bomba, Muszyński 1980; Muszyński, Skowroński 1980; Harańczyk 1982). Adularia was also found in the igneous rocks of this area: diabases (Juskowiak, Ryka 1964; Ryka 1974; Heflik, Muszyński 1983), granodiorites (Banaś *et al.* 1972; Banaś, Piekarski 1978), and in the rocks of the rhyolite-dacite group (Juskowiak, Ryka 1964; Banaś *et al.* 1972; Harańczyk 1982).

A preliminary description of adularia from the basement near Zawiercie was given by Muszyński and Skowroński (1980). The detailed studies of this mineral were carried out on samples derived from four boreholes: WB-9, WB-112, Pz-9 and A-4 (Fig. 1). These were samples: WB-9/8 (taken at a depth of 240 m), Pz-9/27 (554.5 m), Pz-9/31 (579.5 m), WB-112/21 (479 m), A-4/32 (538 m). They were taken

* Institute of Geology and Mineral Deposits, Academy of Mining and Metallurgy in Cracow (Kraków, al. Mickiewicza 30).

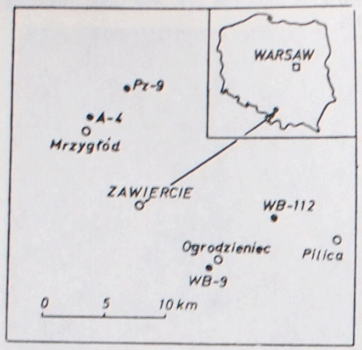

Fig. 1. The location of boreholes from which samples of mineral veins with adularia were taken for mineralogical investigations

from veinlets occurring in poorly altered clay-clastic Silurian rocks. Adularia was subjected to macro- and microscopic studies, X-ray diffraction, infrared spectroscopic and electron microprobe analyses.

EXPERIMENTAL

X-ray powder patterns were recorded with a DRON-1.5 diffractometer, using filtered CuK_α radiation. Infrared absorption spectra were obtained with a Carl Zeiss-Jena UR-10 spectrometer, using KBr discs. These investigations were carried out on adularia fractions separated by hand under the stereoscopic microscope. Prior to separation, the ground vein matter was hot-treated with a 10% HCl solution to remove carbonate minerals. Because of the small size (a few mm) of veinlets and adularia crystals and their intergrowths with the other components of the veinlets, the preparation of an adequate amount of adularia fraction presented considerable difficulties. Therefore, adularia fraction was separated only from the samples WB-9/8, Pz-9/31 and WB-112/21.

Chemical determinations were made on an ARL SEMQ electron microprobe operated at an accelerating voltage of 20 kV and a sample current of 15 nA. The material to be investigated was prepared in the form of polished sections made from fragments of veinlets with adularia sealed in the Epidian organic resin. To give a conductive surface, the samples were coated with a thin (about 100 Å) layer of gold. Adularia grains were analysed for K, Na, Ba, Ca and Fe, using complex standards only. K was determined using KH_2PO_4, Na — synthetic glass (its composition: 71.62 wt.% SiO_2, 1.32 wt.% Al_2O_3, 0.15 wt.% Fe_2O_3, 8.70 wt.% CaO, 3.75 wt.% MgO, 13.85 wt.% Na_2O), Ba—BaF_2 or $BaSO_4$, Ca—CaF_2 or $CaCO_3$, Fe—FeS_2. The content of these elements was determined from the intensity of the K_α line, and only barium content was determined from the intensity of the L_α line. The calculations were corrected for absorption and atomic number difference. Since X-ray fluorescence in the material studied was insignificant, a correction for this effect was omitted from the calculations.

RESULTS

Macro- and microscopic studies

The adularia studied occurs in fissure veinlets (Phot. 1) in paragenesis with quartz and calcite, being usually accompanied by subordinate Mg—Fe-chlorites and unidentified ore minerals.

In similar parageneses, noted however in other boreholes, ore minerals are generally represented by pyrite, chalcopyrite, sphalerite, molibdenite, and sporadically by Bi and W minerals (Łydka 1971; Bukowy, Ślósarz 1975; Harańczyk 1979; Ciemniewska 1978; Ziętek-Kruszewska 1980). In the samples studied adularia is older than quartz and calcite, as its crystals grew directly on the side walls of fissures, and quartz and calcite crystallized successively on these crystals (Phot. 2).

Macroscopically adularia is usually transparent, colourless or grey, little differing from the accompanying quartz. Sometimes it has a pale-pink colour, which makes it similar to carbonate minerals. Adularia crystals are small, generally up to 1 mm, attaining a maximum size of 2 mm. Viewed under the microscope, they sometimes show a habit of short prisms with the cross-section close to a rhomb.

The most pronounced diagnostic feature of adularia under the microscope is its optical heterogeneity. It manifests itself in the sector-zonal structure and spotted or wavy extinction (Phot. 2). Characteristic are also the orthorhombic habits of idio- and hipidiomorphic adularia crystals, observed commonly in thin sections. These crystals often form microdruses at the edges of veinlets (Phot. 2). Adularias may also form irregular xenomorphic grains and then they look exactly like quartz. Viewed under the microscope, fine, xenomorphic crystals of adularia are also hardly distinguishable from albite. However, any doubts can be readily dispelled by conoscopic studies. Adularia crystals usually resemble interference patterns typical of optically negative uniaxial minerals. This is because the adularias studied have a small optic axial angle, usually from some to a dozen or so degrees, at the most amounting to about 40°. This feature indicates that the degree of structural ordering of these minerals is low to intermediate. It corresponds to sanidine, the intermediate members between sanidine and orthoclase, and exceptionally to orthoclase.

Adularia in the veinlets is usually fresh, being only sometimes replaced by kaolinite, sericite and/or muscovite and calcite. It contains scarce inclusions of wall rock components, early-crystallized chlorites and ore minerals.

X-ray and IR spectroscopic investigations

The X-ray diffraction patterns obtained for the adularias (Fig. 2) are typical of K-feldspars with a low or, at most, medium degree of ordering of Si/Al in their crystal lattice. This is evidenced by the sharp *130* and *131* reflections, which show no tendency to split. The projection points plotted onto Wright's diagram (1968) on the basis of the obtained data (Tab. 1) fall in the "high-sanidine" — "Benson" orthoclase area. From the structural point of view, the closest to sanidine is adularia from the sample WB-112/21, and the closest to orthoclase — adularia from the sample Pz-9/31. The feldspars under study have normal dimensions of the unit cell. Owing to this, it is possible to determine the content of the albite component from the $\bar{2}01$

Table 1

Data for the determination of the structural state and composition of adularias by Wright's method (1968)

hkl	Sample					
	Pz-9/31		WB-9/8		WB-112/21	
	2Θ	% Ab	2Θ	% Ab	2Θ	% Ab
$\bar{2}01$	20.95	5	20.96	0	20.95	0
060	41.67		41.64		41.54	
$\bar{2}04$	50.71		50.74		50.80	

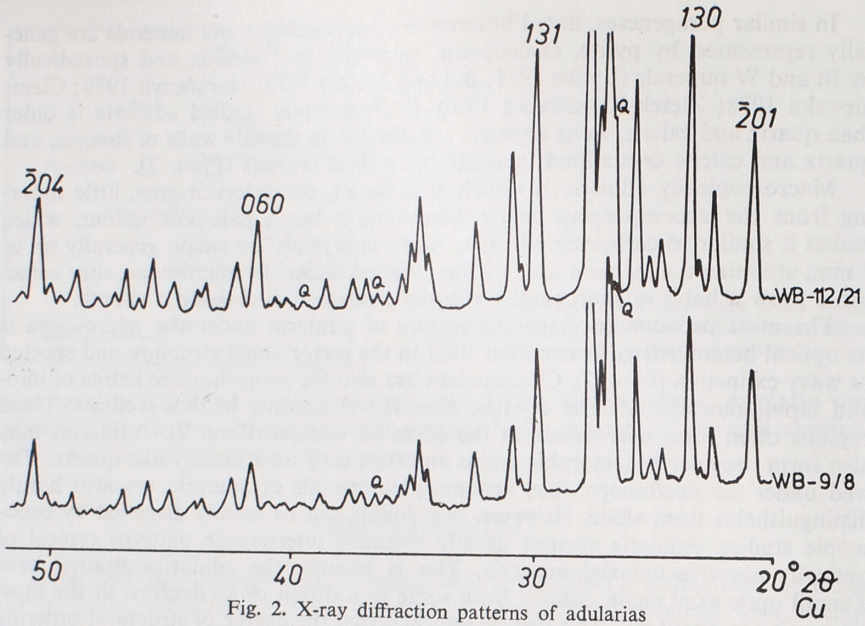

Fig. 2. X-ray diffraction patterns of adularias
Q — reflections from a quartz admixture

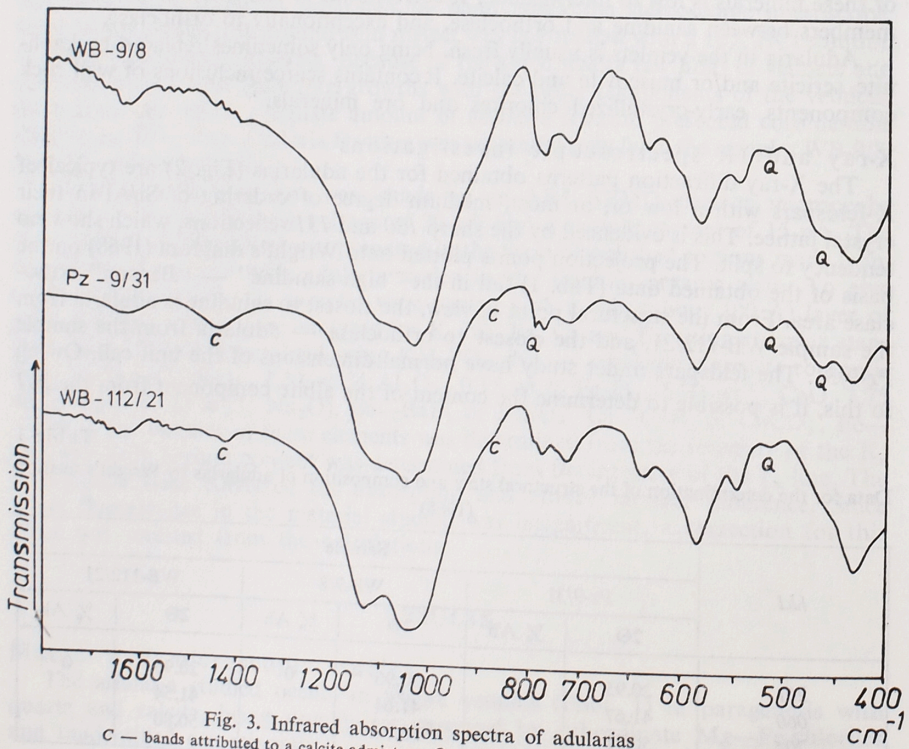

Fig. 3. Infrared absorption spectra of adularias
C — bands attributed to a calcite admixture, *Q* — bands attributed to a quartz admixture

Table 2

Wave numbers (cm^{-1}) of infrared absorption bands of adularias

Sample		
Pz-9/31	WB-9/8	WB-112/21
—	413	407
429	430	430
541	543	544
586	582	584
640	637	639
727	729	727
779	780	779
1017	1017	—
1051	1043	1037
1127	1127	1132

reflection and Wright's diagram. It was found that the adularias studied either contain no albite component or its content seldom rises above 5% Ab.

The infrared absorption spectra of the adularias (Fig. 3, Tab. 2) point again to the low or medium degree of order. This can be inferred from the general diffusion of bands, particularly in the range 700—800 cm^{-1}, as well as from the presence of only two distinct bands (sometimes accompanied by a third, weak inflexion) in the region of ν_3 stretching vibrations (900—1200 cm^{-1}), and the low intensity of the 730 cm^{-1} band (Hafner, Laves 1957). Moreover, the studies of Černy and Chapman (1984) have shown that the shape of the curve and the position of some absorption bands in the range 15.0—19.0 μm (666.7—526.3 cm^{-1}) change in response to the change in the degree of structural ordering of K-feldspars. For adularia from

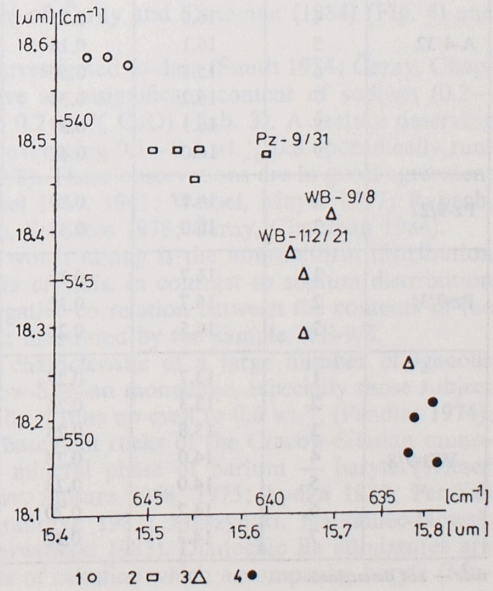

Fig. 4. The position of projection points for adularias from the samples Pz-9/31, WB-9/8 and WB-112/21 on the diagram of Černy and Chapman (1984), and the points for adularias with the following structures distinguished by these authors *1* — of maximum microcline, *2* — of orthoclase with subordinate intermediate microcline, *3* — of high-sanidine with subordinate intermediate microcline, *4* — of high-temperature sanidine

the sample WB-112/21 characteristic are the 544 and 639 cm^{-1} bands, while for adularia from the sample Pz-9/31 — the 541 and 639 cm^{-1} bands. It appears, therefore, that the former shows the closest similarity to high-sanidine with subordinate intermediate microcline (Černy, Chapman 1984), whereas the latter — to orthoclase with subordinate intermediate microcline (Fig. 4).

Chemical determinations

Some of the samples (A-4/32, Pz-9/27, Pz-9/31, WB-9/8) were analysed by electron microprobe. Data for all of the analysed sites were presented in the table 3. Distribution some of these sites show photographs 4a, 5a, 6a.

It was found that the adularia present in them is characterized by a low content of CaO, Na_2O and BaO (Tab. 3). In addition, Fe_2O_3 content was determined for pale-pink adularia from the Pz-9/31 sample and was found to run up to 0.1 wt.% (Tab. 3). However, the distribution of iron in the analysed crystal is not uniform, presumably due to the presence of submicroscopic concentrations of haematite. This mineral is very likely responsible for the pale-pink colour observed macroscopically in adularia from the sample Pz-9/31.

Potassium content in the adularia crystals is close to theoretical for K-feldspars, varying from 13.3 to 16.7 wt.% K_2O (Tab. 3). The lowest potassium contents are

Table 3

Electron microprobe analysis of adularias

Sample	Number of analysed site	Content of components (wt %)				
		K_2O	Na_2O	CaO	BaO	Fe_2O_3
A-4/32	1	15.6	0.29	0.11	0.18	n.d.
	2	15.8	0.31	0.14	0.15	n.d.
	3	16.0	0.21	0.05	0.25	n.d.
	4	16.0	0.25	0.14	0.14	n.d.
	5	16.1	0.18	0.07	0.19	n.d.
	6	15.8	0.50	0.10	0.14	n.d.
	7	16.2	0.34	0.21	0.05	n.d.
	8	16.1	0.37	0.14	0.14	n.d.
	9	16.0	0.42	0.14	0.09	n.d.
Pz-9/27	1	16.1	0.29	0.07	0.18	n.d.
	2	16.0	0.41	0.17	0.35	n.d.
Pz-9/31	1	16.7	0.30	0.08	0.19	0.12
	2	16.7	0.32	0.15	0.20	0.11
	3	16.5	0.25	0.12	0.19	0.10
WB-9/8	1	13.7	0.27	0.01	0.38	n.d.
	2	13.3	0.24	—	0.97	n.d.
	3	13.8	0.23	0.03	0.52	n.d.
	4	14.0	0.23	0.01	0.90	n.d.
	5	14.0	0.23	0.01	0.83	n.d.
	6	14.2	0.20	0.02	0.71	n.d.
	7	14.3	0.20	0.02	0.36	n.d.

n.d. — not determined.

paralleled by the highest content of sodium, calcium, and especially barium admixtures. In all the analysed samples the content of sodium is similar, between 0.2 and 0.3 wt.%, seldom rising above 0.5 wt.% Na_2O (Tab. 3). The distribution of this element in adularia crystals is uniform (Phots. 3—6). The contents of the Ab component calculated from electron microprobe analyses are in accord with the X-ray data and generally fall within the range 1.5—2.5% Ab, sporadically running up to 4% Ab.

Calcium content in the adularia crystals is lower than that of sodium and does not rise above 0.2 wt.% CaO (Tab. 3). This corresponds to the content of the An component amounting at the most to 1%. The Ca content is obviously the lowest in adularia crystals from the sample WB-9/8, where it is close to the geochemical background of this element. A point of interest is that this sample has the highest barium content. In the analysed crystals calcium shows non-uniform distribution, as illustrated by adularia from the sample A-4 (Phot. 6). It concentrates mainly in the marginal parts of this mineral, on the contact with the neighbouring calcite.

A characteristic feature of adularia in the samples studied is the increased content of barium, even running up to 1.0 wt.% BaO in the sample WB-9/8. In the other samples its content is lower, ranging from 0.1 to 0.3 wt.% BaO. Barium is generally distributed unevenly, as shown by the sample WB-9/8 (Phots. 3, 4).

DISCUSSION AND CONCLUSIONS

In respect of macro- and microscopic features, the adularias studied are typical representatives of this variety of potassium feldspars. Their hipidiomorphic crystals show a pseudo-orthorhombic habit and optical heterogeneity, typical of adularias (Phot. 2).

The results of optical studies, and particularly of X-ray and infrared spectroscopic investigations indicate unequivocally that the degree of structural order of these adularias varies from low to intermediate. This is shown by the position of projection points both on the diagram of Černy and Chapman (1984) (Fig. 4) and on Wright's diagram (1968).

Like all the feldspars of this type investigated to-date (Smith 1974; Černy, Chapman 1984), the adularias studied have an insignificant content of sodium (0.2—0.5 wt.% NaO) and calcium (up to 0.2 wt.% CaO) (Tab. 3). A feature deserving note is the increased barium content, averaging 0.1—0.3 wt.% but sporadically running up to 1 wt.% BaO (sample WB-9/8). These observations are in good agreement with the data of other authors (Weibel 1957, 1961; Weibel, Mayer 1957; Rybach, Nissen 1967; Smith 1974; Dimitriadis, Soldatos 1978; Černy, Chapman 1984).

As regards subordinate elements, worth noting is the non-uniform distribution of calcium and barium in the adularia crystals, in contrast to sodium distribution (Phots. 3, 4, 6). There is a distinct negative correlation between the contents of the two former components (Tab. 3), best illustrated by the sample WB-9/8.

The increased barium content is characteristic of a large number of igneous rocks from the basement of the Cracow-Silesian monocline, especially those subject to hydrothermal alteration. Sporadically it runs up even to 0.6 wt.% (Pendias 1974). In the mineral veins crosscutting the basement rocks of the Cracow-Silesian monocline there often appears a separate mineral phase of barium — baryte (Wieser 1957; Juskowiak, Ryka 1964; Bukowy, Ślósarz 1968, 1975; Łydka 1973; Pendias 1974; Ryka 1974; Ślósarz 1979; Harańczyk 1982; Muszyński, Natkaniec-Nowak 1982; Ślósarz *et al.* 1982; Ślósarz, Karwowski 1983). Diadochic Ba admixtures are presumably also present in the crystals of celestine which accompanies baryte (Mu-

szyński, Natkaniec-Nowak 1982; Ślósarz, Karwowski 1983). The adularia under study is, therefore, another mineral from the basement of the Cracow-Silesian monocline, in which barium concentration has taken place.

Acknowledgements. The authors wish to express their thanks to Professor Tadeusz Wieser for the critical reading of the manuscript, and to Mr Andrzej Janas for electron microprobe analyses.

Translated by Hanna Kisielewska

REFERENCES

BANAŚ M., PAULO A., PIEKARSKI K., 1972: O mineralizacji miedziowej i molibdenowej w rejonie Mrzygłodu. *Rudy Met. Nieżel.* 17, 3—7.

BANAŚ M., PIEKARSKI K., 1978: Mineralizacja polimetaliczna w utworach staropaleozoicznych w obszarze Mrzygłód—Myszków. *Pr. Inst. Geol.* 83, 159—161.

BOMBA M., MUSZYŃSKI M., 1980: Przejawy mineralizacji w skałach sylurskich okolic Ogrodzieńca (monoklina śląsko-krakowska). *Zesz. Nauk. AGH — Geologia* 6, 53—63.

BUKOWY S., ŚLÓSARZ J., 1968: Wyniki wiercenia Bębło koło Ojcowa. *Biul. Inst. Geol.* 212, 7—38.

BUKOWY S., ŚLÓSARZ J., 1975: Profil paleozoiku i mezozoiku w Smoleniu koło Pilicy. *Biul. Inst. Geol.* 282, 419—448.

CIEMNIEWSKA M., 1978: Nowe dane o osadach syluru okolic Mrzygłodu—Zawiercia, *Prz. Geol.* 8, 480—484.

ČERNY P., CHAPMAN R., 1984: Paragenesis, chemistry and structural state of adularia from granitic pegmatites. *Bull. Mineral.* 107, 369—384.

DIMITRIADIS S., SOLDATOS K., 1978: Optical and structural properties of adularia from Xanthi and Ouranoupolis, Greece, and their origin. *N. Jb. Miner. Abh.* 133, 88—105.

HAFNER S., LAVES F., 1957: Ordnung/Unordnung und Ultrarot-Absorption. II. Variation der Lage und Intensität einiger Absorptionen von Feldspäten. Zur Struktur von Orthoklas und Adular. *Z. Krist.* 103, 204—225.

HARAŃCZYK C., 1978: Mineralizacja polimetaliczna w utworach paleozoicznych wschodniego obrzeżenia Górnośląskiego Zagłębia Węglowego. *Pr. Inst. Geol.* 83, 171—184.

HARAŃCZYK C., 1979: Metallogenic evolution of the Silesia-Cracow Region. *Pr. Inst. Geol.* 95, 109—132.

HARAŃCZYK C., 1982: Mineralizacja paleozoiczna północnego i wschodniego obrzeżenia Górnośląskiego Zagłębia Węglowego. Przew. 54 Zjazdu Pol. Tow. Geol., 26—38.

HEFLIK W., MUSZYŃSKI M., 1983: Zmienione diabazy z okolicy Zawiercia. *Kwart. Geol.* 27, 709—722.

JUSKOWIAK O., RYKA W., 1964: Przeobrażenia skał magmowych z północno-wschodniego obrzeżenia Zagłębia Górnośląskiego. *Kwart. Geol.* 8, 398—399.

ŁYDKA K., 1971: Litostratygrafia dolnego paleozoiku rejonu Mrzygłodu i Kotowic. *Kwart. Geol.* 15, 708—709.

ŁYDKA K., 1973: Młodszy prekambr i sylur rejonu Myszkowa. *Kwart. Geol.* 17, 700—709.

MUSZYŃSKI M., NATKANIEC-NOWAK L., 1982: Celestyn i baryt w żyłach mineralnych z paleozoicznego podłoża okolic Zawiercia. *Spraw. Pos. Kom. Oddz. PAN w Krakowie.* Lipiec — grudzień 1980, 24/2, 398—399.

MUSZYŃSKI M., SKOWROŃSKI A., 1980: Niekruszcowe składniki żył mineralnych w skałach staropaleozoicznego podłoża okolicy Zawiercia—Wolbromia. *Kwart. Geol.* 24, 503—520.

PENDIAS H., 1974: Charakterystyka geochemiczna skał magmowych północno-wschodniego obrzeżenia Górnośląskiego Zagłębia Węglowego. *Biul. Inst. Geol.* 278, 5—28.

RYBACH L., NISSEN H. U., 1967: Zerstörungfreie Simultanbestimmung von Na, K und Ba in Adular mittels Neutronaktivierung. *Schweiz. Mineral. Petr. Mitt.* 47, 189—197.

RYKA W., 1974: Asocjacja diabazowo-lamprofirowa północno-wschodniego obrzeżenia Górnośląskiego Zagłębia Węglowego. *Biul. Inst. Geol.* 278, 35—69.

SMITH J. V., 1974: Feldspar Minerals. II. Chemical and textural properties. Springer—Verlag, New York.

ŚLÓSARZ J., 1979: Zonalność mineralizacji miedziowo-molibdenowej w rejonie Myszkowa. *Kwart. Geol.* 23, 479.

ŚLÓSARZ J., KARWOWSKI Ł., 1983: Fizykochemiczne warunki mineralizacji polimetalicznej w utworach paleozoicznych rejonu Myszkowa (NE obrzeżenie Górnośląskiego Zagłębia Węglowego). *Arch. Miner.* 39, 93—108.

SLÓSARZ J., TRUSZEL M., ZIĘTEK-KRUSZEWSKA A., 1982: Charakterystyka mineralogiczno-petrograficzna mineralizacji paleozoiku. Przew. 54 Zjazdu Pol. Tow. Geol., 159—168.

WEIBEL M., 1957: Zum Chemismus der alpinen Adulare II. *Schweiz. Mineral. Petr. Mitt.* 37, 545—553.

WEIBEL M., 1961: Chemische Untersuchungen an alpinen Kluftmineralien. *Schweiz. Mineral. Petr. Mitt.* 41, 8—11.

WEIBEL M., MAYER F., 1957: Zum Chemismus der alpinen Adulare I. *Schweiz. Mineral. Petr. Mitt.* 37, 153—158.

WIESER T., 1957: Charakterystyka petrograficzna albitofirów, porfirów i diabazów z Mrzygłodu w okolicy Zawiercia. *Kwart. Geol.* 1, 113—126.

WRIGHT T. L., 1968: X-ray and optical study of alkali feldspar. II. An X-ray method for determining the composition and structural state from measurement of 2 Θ values for three reflections. *Amer. Miner.* 53, 88—104.

ZIĘTEK-KRUSZEWSKA A., 1980: Mineralizacja polimetaliczna w utworach podłoża paleozoicznego w rejonie Myszkowa. *Kwart. Geol.* 24, 942.

Marek MUSZYŃSKI, Piotr WYSZOMIRSKI

ADULAR Z PODŁOŻA MONOKLINY ŚLĄSKO-KRAKOWSKIEJ OKOLIC ZAWIERCIA

Streszczenie

Badano kryształy adularu występujące w żyłkach przecinających zmienione skały osadowe monokliny śląsko-krakowskiej w okolicach Zawiercia. Występują one w paragenezie z kwarcem i kalcytem, często w towarzystwie podrzędnych ilości Mg—Fe-chlorytów oraz minerałów rudnych głównie Fe, Cu, Zn, Mo. Badane adulary są minerałami o zmiennym stopniu uporządkowania struktury — od niskiego do średniego. Zawartość cząsteczki Ab wynosi w nich 1,5—2,5% (sporadycznie ok. 4%), zaś cząsteczki An — z reguły jest znacznie mniejsza od 1%. Cechą charakterystyczną badanych kryształów adularu jest występowanie w nich diadochowych domieszek baru. Na ogół mieszczą się one w granicach 0,1—0,3% wag. BaO. Sporadycznie zawartość tego składnika dochodzi do ok. 1% wag. BaO. Badany adular stanowi przykład kolejnego — po barycie — minerału z podłoża monokliny śląsko-krakowskiej, w którym ma miejsce koncentracja baru.

OBJAŚNIENIA FIGUR

Fig. 1. Szkic rozmieszczenia otworów wiertniczych, z których pobrano próbki żył mineralnych z adularem do badań mineralogicznych

Fig. 2. Dyfraktogramy rentgenowskie adularów
Q — refleksy pochodzące od domieszki kwarcu

Fig. 3. Krzywe absorpcyjne w podczerwieni adularów
C — pasma pochodzące od domieszki kalcytu, *Q* — pasma pochodzące od domieszki kwarcu

Fig. 4. Położenie punktów projekcyjnych adularów z próbek Pz-9/31, WB-9/8 i WB-112/21 na diagramie Černego i Chapmana (1984) z wyróżnionymi przez tych autorów adularami o strukturze:
1 — mikroklinu maksimum, *2* — ortoklazu z podrzędnym udziałem mikroklinu średniotemperaturowego, *3* — sanidynu wysokotemperaturowego z podrzędnym udziałem mikroklinu średniotemperaturowego, *4* — sanidynu wysokotemperaturowego

OBJAŚNIENIA FOTOGRAFII

Plansza I

Fot. 1. System żyłek szczelinowych, adularowo-kwarcowo-kalcytowych w metamułowcu. Próbka Pz-9/31. Polaroidy skrzyżowane, pow. ok. 50×

Fot. 2. Optycznie niejednorodne kryształki adularu o charakterystycznym, rombowym pokroju w żyłce adularowo-kwarcowo-kalcytowej w metamułowcu. Próbka Pz-9/27. Polaroidy skrzyżowane, pow. ok. 90×

Ad — adular, *C* — kalcyt, *Q* — kwarc.

Plansza II

Fot. 3. Adular z wrostkami kwarcu (Q) w żyłce chlorytowo-adularowo-kwarcowo-kalcytowe z metapiaskowca. Próbka WB-9/8

a — elektronowy obraz topograficzny, *b* — obraz scanningowy KK_α, *c* — obraz scanningowy NaK_α, *d* — obraz scanningowy BaL_α. Wielkość obrazu: 145×110 μm

Plansza III

Fot. 4. Adular w żyłce chlorytowo-adularowo-kwarcowo-kalcytowej z metapiaskowca. Próbka WB-9/8

a — elektronowy obraz topograficzny z naniesionymi numerami punktów analitycznych, *b* — obraz scanningowy KK_α, *c* — obraz scanningowy NaK_α, *d* — obraz scanningowy BaL_α, *e* — obraz scanningowy CaK_α. Wielkość obrazu: 60×47 μm

Plansza IV

Fot. 5. Adular w żyłce adularowo-kwarcowo-kalcytowej z metapiaskowca. Próbka Pz-9/31

a — elektronowy obraz topograficzny z naniesionymi numerami punktów analitycznych, *b* — obraz scanningowy KK_α, *c* — obraz scanningowy NaK_α, *d* — obraz scanningowy CaK_α, *e* — obraz scanningowy FeK_α. Wielkość obrazu: 72×56 μm.

Plansza V

Fot. 6. Adular w żyłce chlorytowo-adularowo-kwarcowo-kalcytowej z metazlepieńca. Próbka A-4/32

a — elektronowy obraz topograficzny z naniesionymi numerami punktów analitycznych, *b* — obraz scanningowy KK_α, *c* — obraz scanningowy NaK_α, *d* — obraz scanningowy BaL_α, *e* — obraz scanningowy CaK_α Wielkość obrazu: 110×85 μm.

Марек МУШИНЬСКИ, Петр ВЫШОМИРСКИ

АДУЛЯР ИЗ ФУНДАМЕНТА СИЛЕЗСКО-КРАКОВСКОЙ МОНОКЛИНАЛИ В ОКРЕСТНОСТЯХ Г. ЗАВЕРЦЕ

Резюме

Исследовались кристаллы адуляра из прожилков, секущих измененные осадочные породы Силезско-Кракевской моноклинали в окрестностях г. Заверце. Они встречаются в парагенезе с кварцем и кальцитом, часто в сопровождении подчиненного количества Mg-Fe-хлоритов, а также минералов

рудных, главным образом Fe, Cu, Zn, Mo. Изучаемые адуляры являются минералами с переменной — от низкой к средней — степенью упорядоченности структуры. Содержание частицы Ab составляет в них 1,5—2,5% (в единичных случаях около 4%), а содержание частицы An как правило меньше 1%. Характерной чертой изучаемых кристаллов адуляра является присутствие в них изморфных примесей бария. В среднем они составляют 0,1—0,3 вес. % BaO. Спорадически содержание этого компонента достигает около 1 вес. % BaO. Изучаемый адуляр является примером очередного, после барита, минерала из фундамента Силезско-Краковской моноклинали, в котором имеет концентрация бария.

ОБЪЯСНЕНИЯ К ФИГУРАМ

Фиг. 1. Схематическая карта размещения буровых скважин, из которых были отобраны образцы минеральных прожилков с адуляром на минералогические исследования

Фиг. 2. Рентгеновские дифрактограммы адуляров

Q — отражения вызванные примесью кварца

Фиг. 3. ИК-кривые поглощения адуляров

C — полосы, образованные примесью кальцита, *Q* — полосы, поисходящие от примеси кварца

Фиг. 4. Положение проекционных точек адуляров из образцов Pz-9/31, WB-9/8 и WB-112/21 на диаграмме Черного и Чапмана (1984) с выделенными этими авторами адулярами со структурой

1 — максимального микроклина, *2* — ортоклаза с подчиненным содержанием среднетемпературного микроклина, *3* — высокотемпературного санидина с подчиненным содержанием среднетемпературного микроклина, *4* — высокотемпературного санидина

ОБЪЯСНЕНИЯ К ФОТОГРАФИЯМ

Таблица I

Фот. 1. Система адуляр-кварц-кальцитовых прожилков в метаалевролите. Образец Pz-9/31. Скрещенные поляроиды. Увел. около 50×

Фот. 2. Оптически неоднородные кристаллики адуляра с характерным ромбическим габитусом в адуляр-кварц-кальцитовом прожилке в метаалевролите. Образец Pz-9/27. Скрещенные поляроиды. Увел. около 90×

Ad — адуляр, *C* — кальцит, *Q* — кварц

Таблица II

Фот. 3. Адуляр с включениями кварца (Q) в хлорит-адуляр-кварц-кальцитовом прожилке в метапесчанике. Образец WB-9/8

a — топографическое электронное изображение, *b* — сканированное изображение KK_α, *c* — сканированное изображение $Na\ K_\alpha$, *d* — сканированное изображение BaL_α. Размеры изображения: 145×110 мкм

Таблица III

Фот. 4. Адуляр в хлорит-адуляр-кварц-кальцитовом прожилке в метапесчанике. Образец WB-9/8

a — электронное топографическое изображение с номерами анализированных мест, *b* — сканированное изображение, $K\ K_\alpha$, *c* — сканированное изображение $Na\ K_\alpha$, *d* — сканированное изображение BaL_α, *e* — сканированное изображение $Ca\ K_\alpha$. Размеры изображения: 60×47 мкм

Таблица IV

Фот. 5. Адуляр в адуляр-кварц-кальцитовом прожилке в метапесчанике. Образец Pz-9/31
a — электронное топографическое изображение с номерами анализированных мест, *b* — сканированное изображение KK_α, *c* — сканированное изображение NaK_α, *d* — сканированное изображение CaK_α, *e* — сканированное изображение Fe K_α. Размеры изображения: 72×56 мкм

Таблица V

Фот. 6. Адуляр в хлорит-адуляр-кварц-кальцитовом прожилке в метаконгломерате. Образец A-4/32
a — электронное топографическое изображение с номерами анализированных мест, *b* — сканированное изображение KK_α, *c* — сканированное изображение NaK_α, *d* — сканированное изображение BaL_α, *e* — сканированное изображение CaK_α. Размеры изображения: 110×85 мкм

EXPLANATIONS OF PLATES

Plate I

Phot. 1. The network of adularia-quartz-calcite fissure veinlets from metasiltstone. Sample Pz-9/31 Crossed polaroids, magn. 50×

Phot. 2. Optically heterogeneous adularia crystals with the characteristic orthorhombic habit in an adularia-quartz-calcite veinlet from metasiltstone. Sample Pz-9/27. Crossed polaroids, magn. 90×

Plate II

Phot. 3. Adularia with quartz inclusions (Q) in a chlorite-adularia-quartz-calcite veinlet from metasandstone. Sample WB-9/8
a — topographic electron image, *b* — scanning image KK_α, *c* — scanning image NaK_α, *d* — scanning image BaL_α. The size of pictures 145×110 μm

Plate III

Phot. 4. Adularia in a chlorite-adularia-quartz-calcite veinlet from metasandstone. Sample WB-9/8
a—topographic electron image with numbers of analysed sites, *b* — scanning image KK_α, *c* — scanning image NaK_α, *d* — scanning image BaL_α, *e* — scanning image CaK_α. The size of pictures 60×47 μm

Plate IV

Phot. 5. Adularia in an adularia-quartz-calcite veinlet from metasandstone. Sample Pz-9/31
a — topographic electron image with numbers of analysed sites, *b* — scanning image KK_α, *c* — scanning image NaK_α, *d* — scanning image CaK_α, *e* — scanning image FeK_α. The size of pictures 72×56 μm

Plate V

Phot. 6. Adularia in a chlorite-adularia-quartz-calcite veinlet from metaconglomerate. Sample A-4/32
a — topographic electron image with numbers of analysed sites, *b* — scanning image KK_α, *c* — scanning image NaK_α, *d* — scanning image BaL_α, *e* — scanning image CaK_α. The size of pictures 110×85 μm

Phot. 1

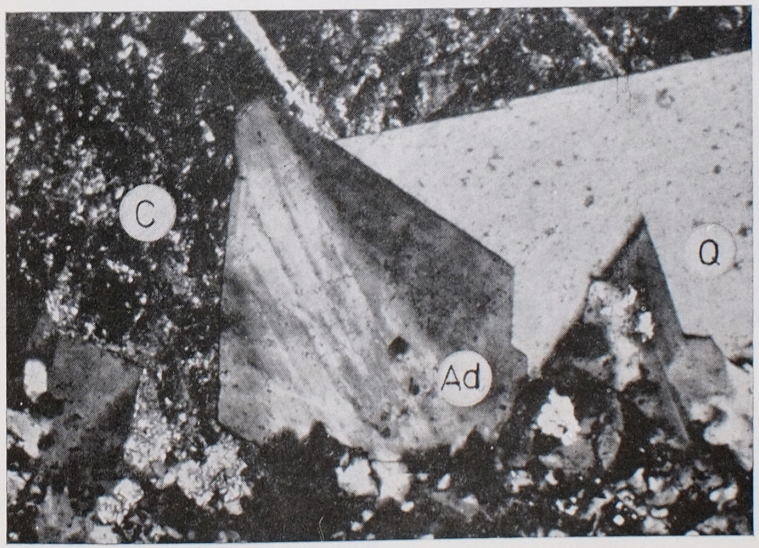

Phot. 2

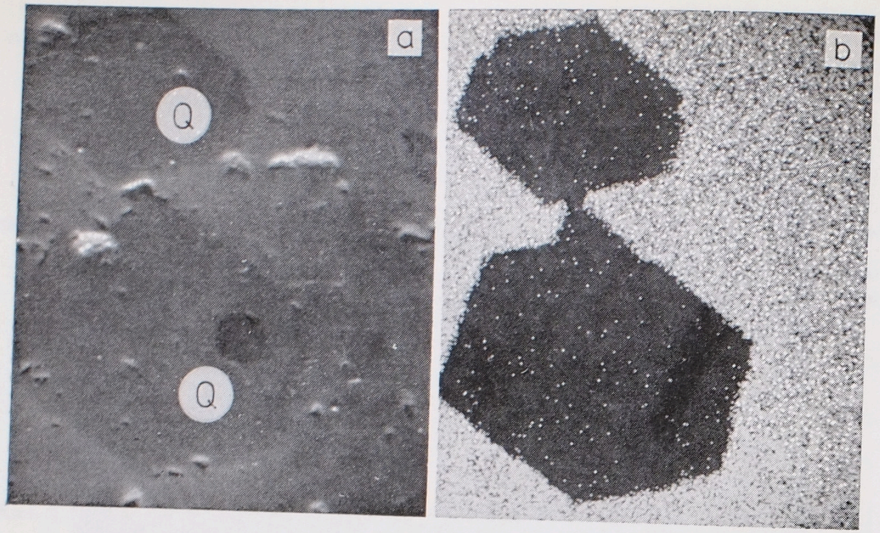

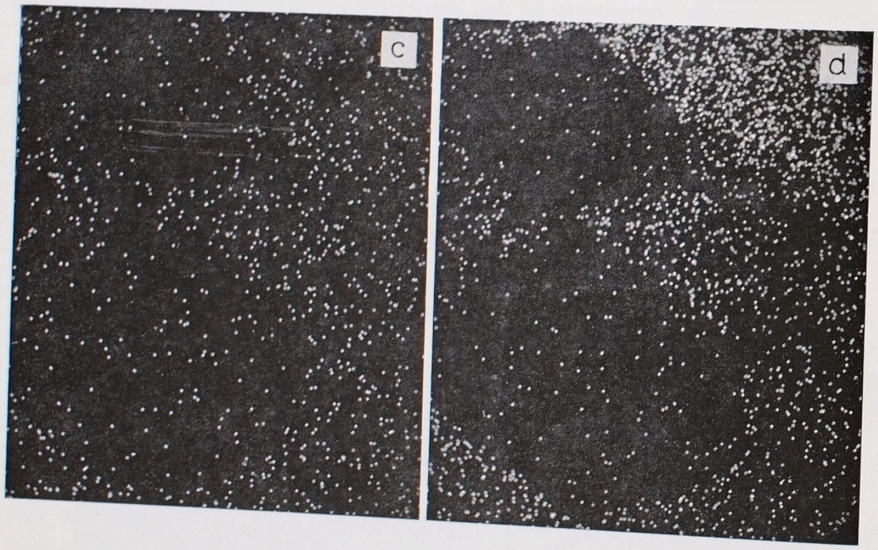

Phot. 3a, b, c, d

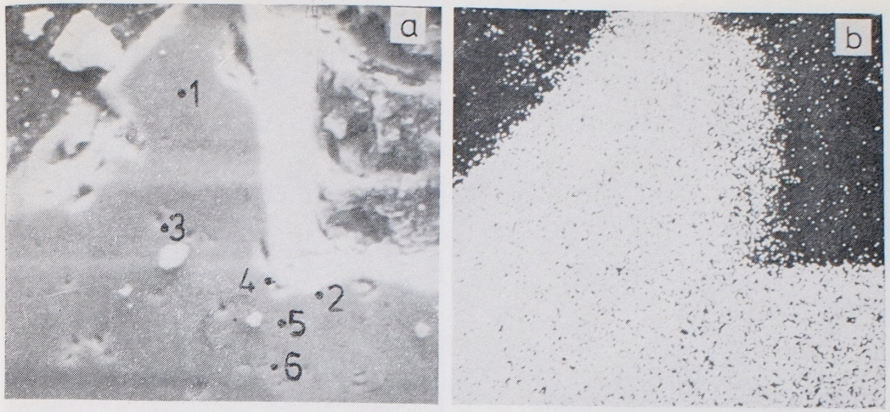

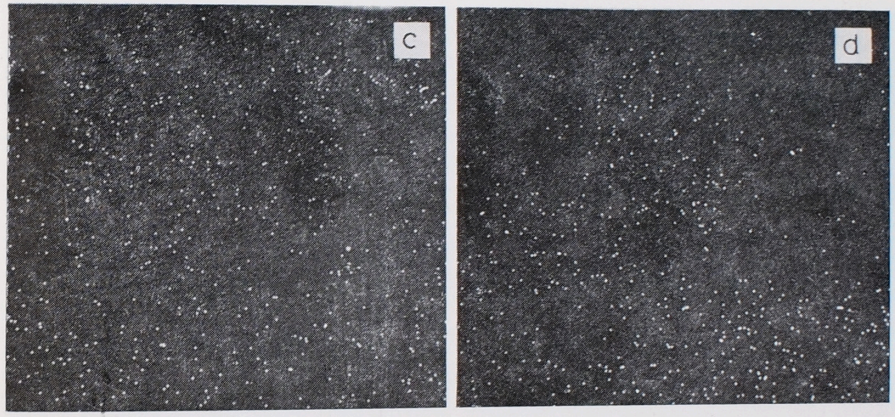

Phot. 4a, b, c, d, e

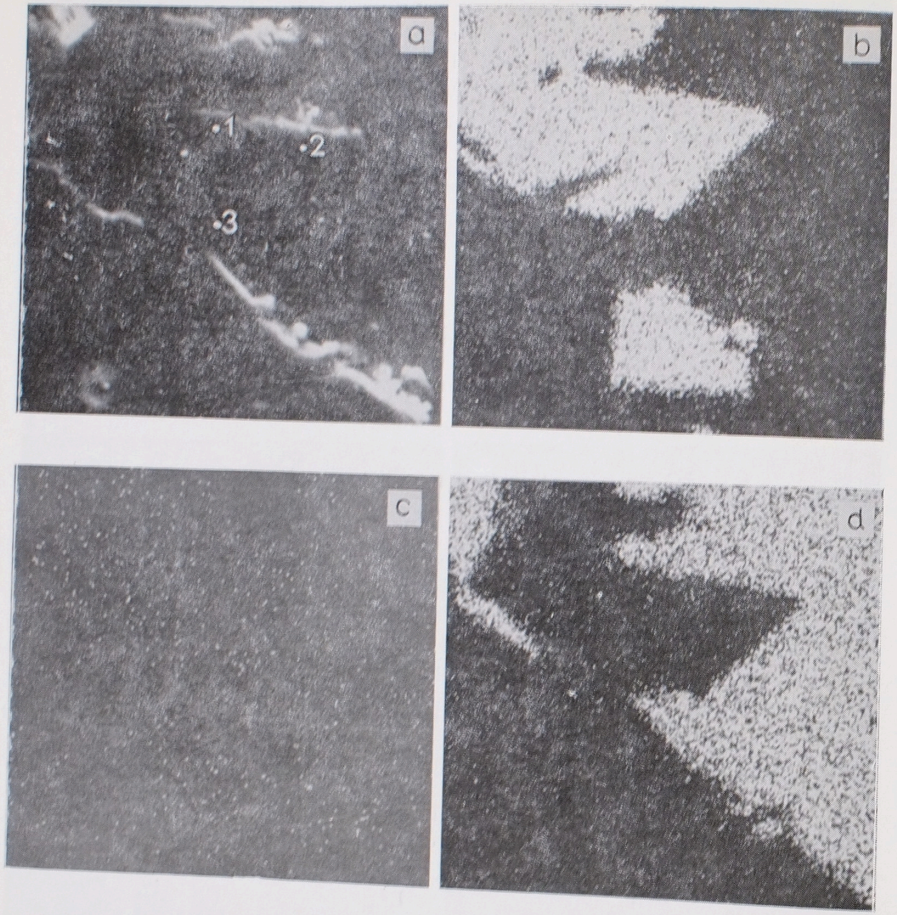

Phot. 5a, b, c, d, e

Marek Muszyński, Piotr Wyszomirski — Adularia from the basement of the Cracow-Silesian Monocline near Zawiercie

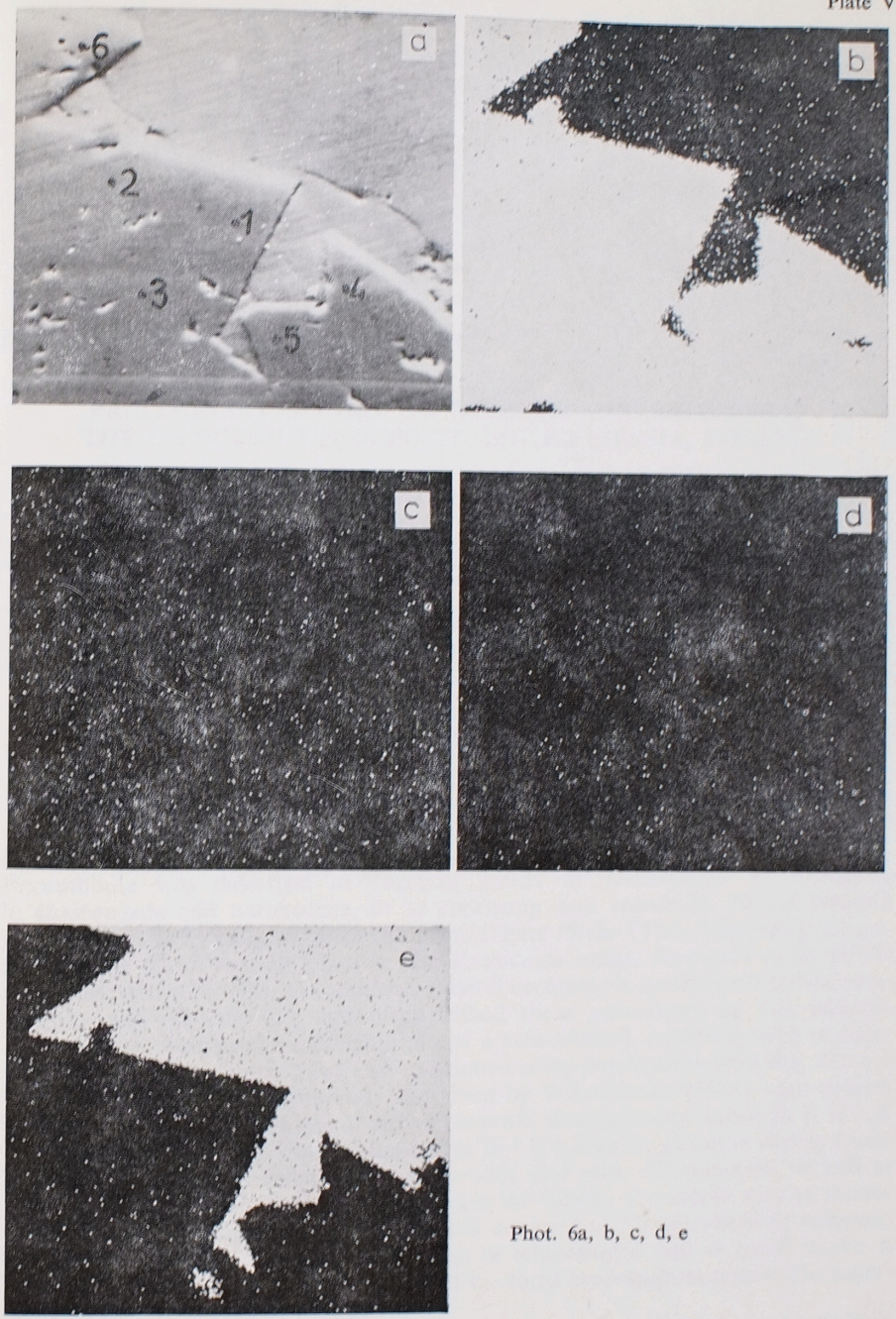

Phot. 6a, b, c, d, e

Marek Muszyński, Piotr Wyszomirski — Adularia from the basement of the Cracow-Silesian Monocline near Zawiercie